

Peak shaving in distribution networks using stationary energy storage systems: A Swiss case study

Nikolaos A. Efkarpidis^{a,*}, Stefano Imoscoli^b, Martin Geidl^a, Andrea Cini^b, Slobodan Lukovic^b, Cesare Alippi^{b,c}, Ingo Herbst^d

^a University of Applied Sciences and Arts Northwestern Switzerland - Institute of Electric Power Systems, 5210 Windisch, Switzerland

^b Università della Svizzera Italiana - The Swiss AI Lab IDSIA, 6962 Lugano, Switzerland

^c Politecnico di Milano - Dipartimento di Elettronica, Informazione e Bioingegneria (DEIB), 20133 Milan, Italy

^d Siemens Switzerland Ltd - Smart Infrastructure Department, 8047 Zürich, Switzerland



ARTICLE INFO

Article history:

Received 25 September 2022

Received in revised form 15 January 2023

Accepted 6 February 2023

Available online 9 February 2023

Keywords:

Battery storage

Peak shaving

Rule-based control

Optimum

Load forecast

ABSTRACT

Grid operators are charged not only by their total energy demand, but also by their highest power demand from the superior grid level. The maximum demand charge is usually imposed on the peak power point of the monthly load profile, hence, shaving demand at peak times is of main concern for the aforesaid stakeholders. In this paper, we present an approach for peak shaving in a distribution grid using a battery energy storage. The developed algorithm is applied and tested with data from a real stationary battery installation at a Swiss utility. This paper proposes a battery storage control scheme that can be used for peak shaving of the total grid load under realistic conditions. Particularly, a rule-based approach combined with a deep-learning load forecasting model is developed and its performance is compared with the theoretical optimum based on real data from the field. The analysis includes both technical and economical results from a simulated storage operation and significant outcomes are given for the application of this method.

© 2023 The Author(s). Published by Elsevier Ltd. This is an open access article under the CC BY license (<http://creativecommons.org/licenses/by/4.0/>).

1. Introduction

1.1. General problem and motivation

Electricity demand, or the energy load, varies over time depending on the season and the load composition, thus, meeting time-varying demand, especially in peak periods, can present a key challenge to electric power utilities [1,2]. Variations in end-customers' daily consumption profiles have created a notable difference in the peaks and valleys of the total load curve, hence, supply and demand balancing or meeting the peak load have become a major concern of utility companies [3,4].

Peak load is a sensitive factor for planning and operation of power grids. Demand peaks impact network planning, since the electrical infrastructure of transmission and distribution (T&D) systems must be designed to support the maximum system demand. However, the T&D infrastructure may be mostly under-utilized, reaching its capacity limit a few times per year. It is evident that a major fraction of the capital and operational grid expenses can result from satisfying its peak power demands. High-demand customers and energy providers are charged not

only by their total energy purchase, but also by their highest power demand that dominates the grid construction costs. The maximum demand charge is usually imposed on the maximum point of the monthly demand profile, thus, reducing demand at peak times is of main concern for grid operators [5]. This is also applied for distribution grids against their superior grid level.

The process of reducing electrical power consumption during periods of high demand is called peak shaving. Utilities adapt the peak loads on the demand side with the end-users' participation [6,7], on the generation side (e.g., dispatchable power plants) and by grid upgrade measures [6,8]. Another possibility is the deployment of battery energy storage systems (BESS): (a) by installing large-scale stationary units at strategic points, e.g., power plants and substations, or, (b) by incentivizing the end-customers to install and control their small-scale units distributed at buildings throughout the grid [9]. BESS currently account for a small portion of energy storage within the grid, however, they gain growing interest owing to their fast ramping time, versatility, high energy density and efficiency, as well as their low O&M cost [10,11]. In Switzerland, a number of stationary BESS are already in operation on behalf of local grid operators [12–14]. The deployed systems provide various services, such as primary frequency response, voltage regulation, energy market balancing and peak shaving. Previous studies concluded that peak shaving is one of the primary services to render a large-scale BESS project

* Corresponding author.

E-mail address: nikolaos.efkarpidis@fhnw.ch (N.A. Efkarpidis).

Nomenclature**Abbreviations**

AC	Alternative Current
BESS	Battery Energy Storage System(s)
DSO	Distribution System Operator
EoL	End of Life
EPEX	European Power Exchange
GRU	Gated Recurrent Unit
MAE	Mean Absolute Error
MAPE	Mean Absolute Percentage Error
MILP	Mixed Integer Linear Programming
MIMO	Multiple-Input Multiple-Output
MLP	Multi-Layer Perceptron
MPC	Model Predictive Control
NLP	Non-Linear Programming
NRMSE	Normalized Root Mean Square Error
O&M	Operating and Maintenance
PV	Photovoltaic
R^2	R-Squared
RNN	Recurrent Neural Network
SGD	Stochastic Gradient Descent
SoC	State of Charge
T&D	Transmission and Distribution
ToUA	Time-of-Use Arbitrage

Superscripts

i	Day of the year, $i \in \{1, 2, \dots, \mathcal{D}\}$
t	Timeslot of the day, $t \in \{1, 2, \dots, \mathcal{T}\}$
min	Minimum
max	Maximum
nom	Nominal

Subscripts

ch	Charge
dis	Discharge
epex	Epex
inv	Inverter
imp	Import
ld	Load
opt	Optimal
peak	Peak
pred	Prediction
rtp	Round-trip
thr	Throughput
tot	Total
use	Use

Sets

\mathcal{T}	Set of time-slots per day
---------------	---------------------------

 \mathcal{D}

Set of days per year

Symbols

α	Year [-]
γ	Power-to-energy rate for charge/discharge [-]
η	Learning rate [-]
θ	Trainable parameters [-]
λ	L2 regularization weight [-]
c	Specific cost of energy [€ MWh ⁻¹]
C	Cost [€]
e	Normalized BESS energy capacity [%]
E	Storage energy content [MWh]
g	Non-linear conditional features [-]
L	BESS annual degradation rate [%]
n	Efficiency [%]
Q	BESS capacity fade [%]
p	Binary variable for BESS power [-]
P	Electric power [MW]
r	Limiting factor [-]
t	Time [hour]
u	Exogenous variables [-]
y	True target for forecasting model [-]
\hat{y}	Predicted output by forecasting model [-]

Hence, it is a challenge for the grid operator to utilize optimally a stationary BESS for peak shaving.

1.2. Literature review

Various representative references from the literature are examined, to understand to which extent they can be applied in use cases of a stationary BESS utilized mainly for peak shaving by the grid operator. Different methods are proposed for peak shaving, either optimization-based or rule-based approaches with the main goal to determine the optimal BESS operation [10,12,17–32].

From the literature review, it is concluded that the existing methods are assessed either at large-scale customer level (such as commercial/industrial facilities and public buildings) [12,17–22] or at regional level (e.g., communities and cities) [10,23–32]. Furthermore, [10,12,17,19,22,27–32] are referred to real-time peak shaving control schemes, while [20,21,23–26] evaluate off-line approaches. One main assumption that is made by various references is to utilize historical load data for the assessment of peak shaving methods without the use of forecasting models [10,12,18,19,21–26,29]. However, real-time peak shaving in distribution networks cannot always be achieved with the proposed control schemes due to the high volatility of network load profiles. Other approaches, which consider fixed power thresholds for activation of the BESS, are not suitable, since peaks in distribution networks are varying from day to day, and from season to season [17,18,20]. Moreover, thresholds that are defined with respect to historical load data may be inaccurate in cases of distribution grids with gradual load variations on seasonal or annual basis [19,21–23,26,29]. Other methods control the BESS based on a load factor that can be predefined for large-scale customers more accurately than for distribution networks [10]. As for the optimization-based methods, optimal peak shaving can be implemented through model predictive control (MPC) [12,27]. These methods are based either on generic consumption patterns [12],

financially viable [15,16]. Focusing on the stationary BESS unit installed in the city of Arbon in Switzerland [14], it is of particular interest to develop a robust BESS control scheme for peak shaving purposes from the network operator's perspective. Particularly, the BESS should achieve peak shaving without increasing the energy procurement costs. Moreover, the robustness of a peak shaving strategy has to be ensured for various load forecasting error levels, since high inaccuracies can lead to low peak reductions.

or on accurate load predictions [27]. In [31], the optimization-based BESS control techniques are also based on accurate load forecasts by aggregating real-time consumption data from the end-customers. Since national regulations rarely allow the real-time monitoring of end-users' energy demand due to privacy issues, this method is not applicable in most countries. Moreover, prediction methods based on the aggregation of load profiles tend to perform poorly when the candidates used are not representative of the total load to be predicted [24]. Other methods aim at load levelling and load smoothing apart from peak shaving, but their performance significantly depends on the accuracy of load prediction [28,30,32]. Finally, in case of inaccurate load forecasts, a smoothing function may also overutilize the BESS and result in high battery degradation [28].

Load forecasting is considered as indispensable part of peak shaving approaches with stationary BESS in distribution grids. In the context of daily load prediction, traditional statistical and autoregressive models, as well as machine learning approaches have been investigated [33]. Recently, deep learning models have emerged as the state-of-the-art method in predicting the future load curve [34], and the future peak consumption [35]. Deep neural networks are able to learn complex non-linear relationships between inputs and prediction targets, which is often cited as an explanation for their better forecasting accuracy [34,36].

From the previous literature review, it is evident that several peak shaving techniques are based on historical load data. Hence, if the actual data deviate from the historical ones, inaccurate charge/discharge commands could cause the increase of peaks rather than reducing them. Moreover, approaches that are based on load forecasts may be too sensitive on load forecasting errors leading to low performance. Besides that, forecasting techniques that are based on the real-time aggregation of individual load profiles may be hindered by the regulatory frameworks due to data privacy and security requirements. Finally, one additional aspect that was not considered in previous publications is the impact of the proposed control schemes on other factors than peak power (or related cost), for example changes in energy procurement cost, and changes in energy-based network usage fees due to peak shaving.

1.3. Approach and main contributions

The main goal of this paper is to evaluate a BESS control scheme that can be used for real-time peak shaving in distribution networks.

The proposed method based on day-ahead load forecasts utilizes not only historical load data, but also near real-time measurements for the total network load at a transformer. Due to the volatile load curve of distribution grids, near real-time transformer measurements can be used to frequently update the power thresholds that are based on the day-ahead peak power predictions. Hence, unsuitable thresholds due to high forecasting errors can be modified, thereby reducing the dependency from the load forecast.

In terms of the load prediction, the impact of different forecasting error levels on the performance of the proposed strategy is also evaluated. This assessment aims to investigate the method robustness on forecast uncertainties.

The study is conducted for a 3.5-year period based on measurement data provided by a Swiss distribution system operator (DSO). In this manner, the method effectiveness can be better ensured compared to the previous publications, which use data sets of shorter periods. The results are compared with the theoretical optimum generated with the actual load data, or in other words, with perfect forecasts and mathematical optimization.

In terms of the economic analysis, it is of main importance for the DSO not only to reduce the peak power cost, but also

not to increase other costs related to energy procurement and energy-based network usage. Consequently, this study includes a comprehensive analysis of all costs for the total 3.5-year period.

In summary, the main contributions of this paper are as follows:

- To which extent a stationary BESS with a rule-based control scheme for peak shaving can achieve cost savings for the DSO in relation to the theoretical optimum.
- Evaluation of strategy robustness examining load prediction forecasts of various accuracy levels.
- Examining to which degree the update frequency of real-time transformer measurements can influence the performance of the method.
- Assessing the influence of BESS control scheme for peak shaving on both peak power and energy procurement costs.

1.4. Structure of the paper

The structure of the paper is organized as follows: Section 2 formulates the problem, specifying the load forecasting model and the control scheme used for the BESS operation. Section 3 presents the pilot implementation, providing the details of the general system layout, as well as the inputs and assumptions considered in the simulations. Next, the results from both the technical and economic assessments are analysed in Section 4. Finally, Section 5 provides a brief summary, and next steps of future work are highlighted.

2. Problem formulation

In this section, first the objective function that is used for the evaluation of the proposed control scheme is defined. Next, the entire system is modelled, followed by the optimal case, as well as the control scheme and the load forecasting method utilized in this study.

2.1. Objective function

The main goal for the DSO is to reduce the power peaks without deteriorating other relevant cost components. The DSO is penalized for the highest monthly 15-min average power exchange with the superior grid level [37]. In order to avoid undesired effects on other cost components, two additional cost factors are considered in the objective function. The total cost C_{tot} consists of three different components:

$$C_{\text{tot}} = C_{\text{epex}} + C_{\text{peak}} + C_{\text{use}} \quad (1)$$

where C_{epex} , C_{peak} and C_{use} represent the total daily cost due to energy purchase, total monthly cost from peak power demand and total daily cost from the usage of transmission and distribution (T&D) networks, respectively. Energy is not purchased by the DSO, and only a small part of the total energy consumption is purchased at the European Power Exchange (EPEX). However, a theoretical total energy cost based on the EPEX prices is included in the objective function, as a worst-case measure for shifts in energy procurement cost due to peak shaving. In this manner, the control schemes are prevented from reducing the peak power cost at the expense of energy procurement and grid usage costs. The individual cost components are:

$$C_{\text{epex}} = \sum_{t=1}^N C_{\text{epex}}(t) E_{\text{imp}}(t) \quad (2)$$

$$C_{\text{peak}} = c_{\text{peak}} \max(P_{\text{ld}}(t)), \quad \forall t \in \{1, 2, \dots, N\} \quad (3)$$

$$C_{\text{use}} = \sum_{t=1}^N c_{\text{use}} E'_{\text{imp}}(t) \quad (4)$$

where N and $P_{\text{ld}}(t)$ are the number of timesteps per day, and power demand at timestep t , respectively. $E_{\text{imp}}(t)$ and $E'_{\text{imp}}(t)$ represent the total energy consumption charged for energy procurement and network usage costs, correspondingly. The penalty factors c_{epex} , c_{peak} and c_{use} are the EPEX day-ahead spot prices, monthly peak power tariff (used on daily basis), and grid usage tariff, respectively.

2.2. System model

The BESS model is formulated considering its main technical constraints. By using the BESS round-trip-efficiency $n_{\text{rtp}}(\alpha)$ at the beginning of year α , it is assumed that the charging and discharging efficiencies, n_{ch} and n_{dis} , respectively, are equal, as follows:

$$n_{\text{ch}} = n_{\text{dis}} = \sqrt{n_{\text{rtp}}(\alpha)} \quad (5)$$

The BESS power $P_{\text{bess}}(t)$ consists of two components, the charging power, $P_{\text{ch}}(t)$ and the discharging power, $P_{\text{dis}}(t)$:

$$P_{\text{bess}}(t) = P_{\text{ch}}(t) - P_{\text{dis}}(t) \quad (6)$$

where the negative sign of $P_{\text{bess}}(t)$ indicates a discharging operation. Both charging and discharging powers are non-negative and constrained by the maximum charging and discharging power limits, which are equal to the ac power rating of the converter, P_{nom} :

$$0 \leq P_{\text{ch}}(t) \leq P_{\text{nom}} \quad (7)$$

$$0 \leq P_{\text{dis}}(t) \leq P_{\text{nom}} \quad (8)$$

The BESS energy content at timestep t depends on the energy content and power at timestep $t - 1$, hence, the following recurrent relation shall be fulfilled:

$$E_{\text{bess}}(t) = E_{\text{bess}}(t - 1) + \Delta t n_{\text{ch}} n_{\text{inv}} P_{\text{ch}}(t) - \frac{\Delta t P_{\text{dis}}(t)}{n_{\text{dis}} n_{\text{inv}}} \quad (9)$$

where Δt is the timestep, n_{inv} is the BESS converter efficiency. As for the limits of energy content, the state of charge $\text{SoC}(t)$, which is defined as the ratio of the energy content at each timestep $E_{\text{bess}}(t)$ to the rated energy capacity, E_{nom} , can be utilized. In particular, the upper and lower SoC bounds, SoC_{max} and SoC_{min} are defined in advance with respect to technical characteristics of the battery, therefore, the following constraints are utilized for the energy content:

$$\text{SoC}_{\text{min}} E_{\text{nom}} \leq E_{\text{bess}}(t + 1) \leq \text{SoC}_{\text{max}} E_{\text{nom}} \quad (10)$$

Apart from the power and energy constraints, the battery degradation $L_{\text{bess}}(\alpha)$ is also calculated at the end of year α . The remaining normalized BESS energy capacity $e_{\text{bess}}(\alpha)$ is provided by:

$$e_{\text{bess}}(\alpha) = L_{\text{bess}}(\alpha) e_{\text{bess}}(\alpha - 1) \quad (11)$$

The main factors that have crucial impact on the battery degradation are the SoC, depth of discharge, charging rate, time, battery temperature, and the cycle type (full or partial). The degradation model developed for Li-ion batteries of lithium manganese oxide (LMO) in [38], is also used in this study. Based on [39], the $n_{\text{rtp}}(\alpha)$ at the end of each year also reduces, as follows:

$$n_{\text{rtp}}(\alpha) = n_{\text{rtp}}(\alpha - 1) - 0.2303Q(\alpha) \quad (12)$$

where $Q(\alpha)$ is the capacity fade, and is provided by:

$$Q(\alpha) = e_{\text{bess}}(\alpha - 1) - L_{\text{bess}}(\alpha) \quad (13)$$

Energy losses, when the BESS is in idle mode, are not considered for the sake of simplicity, since they have negligible impact on the BESS efficiency.

The power equilibrium at the point of common grid coupling for the BESS is given by:

$$P_{\text{imp}}(t) = P_{\text{ld}}(t) + P_{\text{bess}}(t) \quad (14)$$

considering the BESS power $P_{\text{bess}}(t)$, the import power from the upstream network $P_{\text{imp}}(t)$, and the total power of the feeder $P_{\text{ld}}(t)$. The energy $E_{\text{imp}}(t)$ considered in energy costs at each timestep is defined as follows:

$$E_{\text{imp}}(t) = \Delta t P_{\text{imp}}(t) \quad (15)$$

In terms of the network usage costs, the energy required for BESS charging is free of charge in Switzerland, in the same manner as for hydro power plants [37]. Consequently, the energy $E'_{\text{imp}}(t)$ considered in the network usage cost is given by:

$$E'_{\text{imp}}(t) = \Delta t (P_{\text{ld}}(t) - P_{\text{dis}}(t)) \quad (16)$$

where the BESS discharging power is solely used.

2.3. Optimal case

The optimal case is based on a daily optimization for the BESS operation utilizing a perfect load prediction and the results are used as a reference for the evaluation of the proposed control schemes. Regarding the powers, a binary variable $p(t)$ is used to exclude that both charging and discharging powers have a non-zero value:

$$0 \leq P_{\text{ch}}(t) \leq p(t) P_{\text{nom}} \quad (17)$$

$$0 \leq P_{\text{dis}}(t) \leq (1 - p(t)) P_{\text{nom}} \quad (18)$$

It is assumed that the BESS energy content at the first and last timestep of each day are equal to the initial state of charge SoC_0 :

$$E_{\text{bess}}(1) = E_{\text{bess}}(N) = \text{SoC}_0 E_{\text{nom}} \quad (19)$$

The authors are aware that this heuristic assumption represents an additional constraint for the optimization that may lead to sub-optimal solutions. The main reason why the constraint (19) is included is to guarantee the BESS sustainability for the project lifetime. When the energy at the end of each day is not defined, the BESS unit may remain at low SoC levels for long periods, which can considerably increase its degradation. A representative measure of battery life is the energy throughput, which corresponds to the total amount of energy a battery stores over its lifetime. In this study, the daily energy throughput E_{thr} is of main importance, since the optimization is carried out on daily basis:

$$E_{\text{thr}} = \sum_{t=1}^N \Delta t n_{\text{ch}} n_{\text{inv}} |P_{\text{ch}}(t)| \quad (20)$$

Furthermore, a constraint for the daily energy throughput is included in order to limit the BESS degradation:

$$E_{\text{thr}} \leq r_{\text{thr}} E_{\text{nom}} \quad (21)$$

where r_{thr} is predefined according to the desirable daily number of cycles and the utilized SoC range.

In case of repeated power peaks the goal of the optimization is to shave only the highest peak of the current month up to now and not each peak of the day, since only the monthly peak

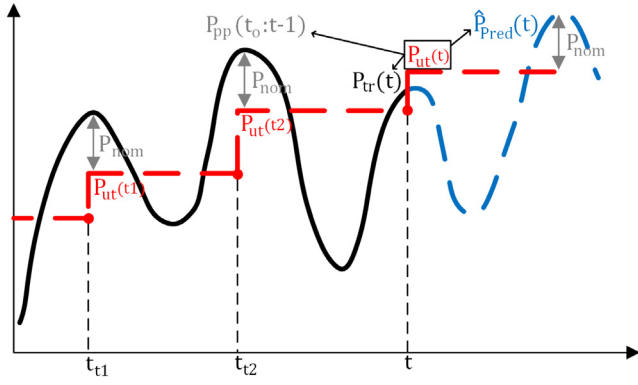


Fig. 1. Concept of rule-based approach for the update of a threshold used for BESS charging and discharging.

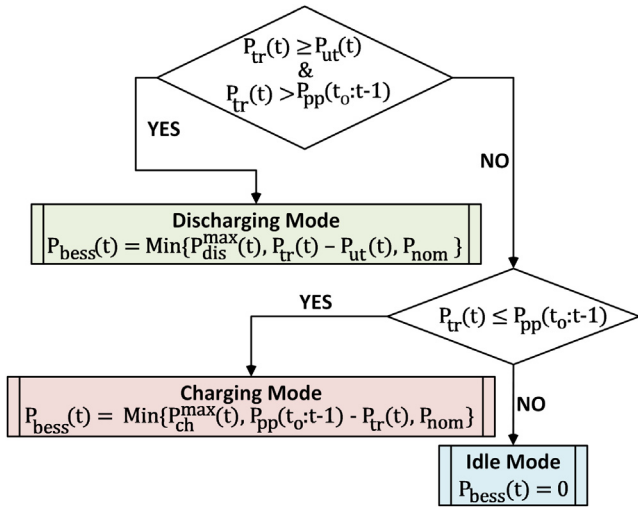


Fig. 2. Logic diagram for the determination of each BESS mode.

is of concern. The constraints (19)–(21) do not limit the BESS operation in the case of rule-based strategy, but they are solely used for the optimal operation, where the load forecasts are ideal.

In summary, the complete optimization problem based on a mixed integer linear programming (MILP) formulation focuses on the minimization of daily C_{tot} and can be expressed as:

$$\begin{aligned} \min \quad & C_{tot} \\ \text{s.t.} \quad & \text{Constraints (1) – (10), (14) – (21)} \\ & \forall t \in \{1, 2, \dots, N\} \end{aligned} \quad (22)$$

The total daily cost does not include the operational costs of BESS installation, e.g., degradation and O&M costs, or other costs related to erection, replacement and system reinforcement. The study aims not to provide an analytical business model for the whole project horizon of BESS investment, but to define the potential of cost savings with peak shaving in a real use case.

2.4. BESS control scheme

The rule-based strategy utilizes a threshold for both the charging and discharging modes of BESS. As shown in Fig. 1, the threshold $P_{ut}(t)$ at timestep t is updated with respect to the monthly peak power of the previous timesteps $P_{pp}(t_0 : t - 1)$, the near real-time transformer measurement $P_{tr}(t)$ and the day-ahead

predicted peak power $\hat{P}_{pred}(t)$. The threshold $P_{ut}(t)$ is calculated every 15 min, as follows:

$$P_{ut}(t) = \text{Max}\{P_{ut}(t - 1), \text{Max}\{\hat{P}_{pred}(t), P_{pp}(t_0 : t - 1), P_{tr}(t)\} - P_{nom}\} \quad (23)$$

The threshold $P_{ut}(t)$ can only remain constant or increase at each timestep compared to the previous threshold $P_{ut}(t - 1)$. In particular, the use of both the previous threshold and the monthly peak power of the previous timesteps can prevent fluctuations of the threshold, avoiding any discharging cycles at local peaks. In addition, the use of the near real-time transformer measurement can lead to the continuous update of the threshold. Within the 15-min time interval, the threshold can also be updated using the latest load prediction, as a new day-ahead load prediction is provided every 15 min. The nominal power P_{nom} is used in (23) so that the BESS charging power is sufficient to reduce the power peak when using the full power capacity.

Fig. 2 provides the logic diagram for the determination of each BESS mode. For the discharging mode, two conditions must be met, particularly, the near real-time load measurement $P_{tr}(t)$ should be equal or higher than the threshold $P_{ut}(t)$, and higher than the monthly peak power of the previous timesteps $P_{pp}(t_0 : t - 1)$. In this manner, the BESS does not discharge at peaks lower than the previous monthly peak exploiting the BESS energy content only when required. In this case, the discharging power is provided by:

$$P_{bess}(t) = \text{Min}\{P_{dis}^{max}(t), P_{tr}(t) - P_{ut}(t), P_{nom}\} \quad (24)$$

where $P_{dis}^{max}(t)$ corresponds to the maximum discharging power at each timestep based on the current SOC(t):

$$P_{dis}^{max}(t) = \frac{E_{nom} n_{dis} n_{inv}}{\Delta t} (SoC(t) - SoC_{min}) \quad (25)$$

It is evident that the BESS does not always discharge with the rated power, P_{nom} , as the difference $P_{tr}(t) - P_{ut}(t)$ may be lower than P_{nom} , or the BESS remaining capacity limits the discharging power.

As for the charging mode, the load measurement $P_{tr}(t)$ should be equal or lower than the monthly peak power of the previous time intervals $P_{pp}(t_0 : t - 1)$. The charging power is given by:

$$P_{bess}(t) = \text{Min}\{P_{ch}^{max}(t), P_{pp}(t_0 : t - 1) - P_{tr}(t), P_{nom}\} \quad (26)$$

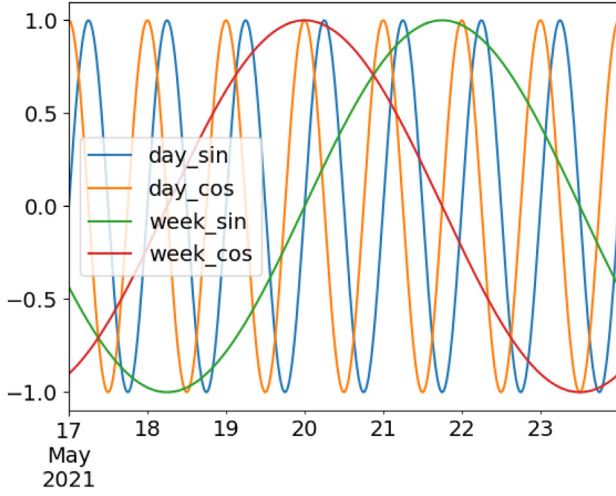
where $P_{ch}^{max}(t)$ represents the charging power at each timestep with respect to the current SOC(t):

$$P_{ch}^{max}(t) = \frac{E_{nom}}{\Delta t n_{ch} n_{inv}} (SoC_{max} - SoC(t)) \quad (27)$$

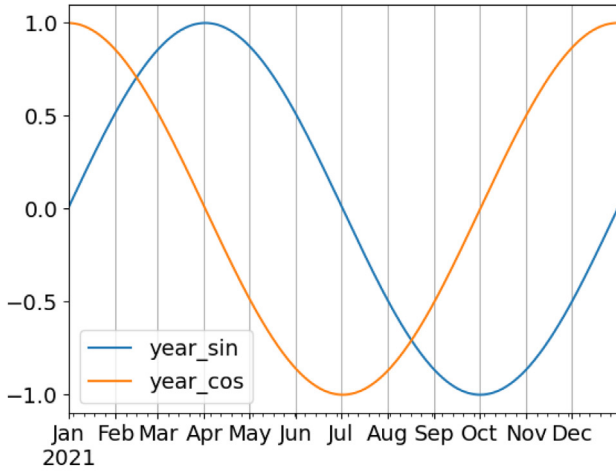
In the same manner to the discharging power, the charging power cannot always be equal to P_{nom} , since the BESS charging mode should not cause higher peaks than the monthly current one $P_{pp}(t_0 : t - 1)$, or the BESS requires lower power to be charged up to the SoC_{max} . It is evident from the aforesaid concept of charging mode that the BESS can be charged very frequently so that there exists sufficient energy capacity to reduce the power peaks in case of discharging mode. Finally, when neither the charging nor the discharging conditions are met, the BESS remains in idle mode.

2.5. Load forecasting model

The BESS operation relies on peak load predictions of the future 24 hours, $\hat{P}_{pred}(t)$, which are updated every 15 min. Based on a recent review of state-of-the-art deep learning models for electric load forecasting [34], we choose Recurrent Neural Networks (RNNs) with Gated Recurrent Unit (GRU) as the core of our prediction system [40,41]. GRUs are a simple version of



(a)



(b)

Fig. 3. Sinusoidal encodings of the timestamps, used as exogenous variables to inform the forecasting model about: (a) weekly and daily periodicity, and (b) seasonal patterns.

gated RNNs, suited for the processing of temporal data. They have already been applied successfully in many load forecasting scenarios [36,42].

Following the results in [34], we employ the Multiple-Input Multiple-Output (MIMO) strategy and use a window of w past observations to predict directly the whole horizon of h future values, with a single pass through the model. At each step t the model receives as input a sequence $\{P_{ld}(t-w+1), \dots, P_{ld}(t-1), P_{ld}(t)\}$ of w past load measurements and a window of corresponding exogenous variables $\{\mathbf{u}(t-w+1), \dots, \mathbf{u}(t-1), \mathbf{u}(t)\}$. These could be extra data (e.g., weather forecasts). In our case, we define $\mathbf{u}(t)$ as a 7-dimensional vector, where the first six variables are sinusoidal encodings of the horizon timestamps, as shown in Fig. 3. The last variable assumes a value of 0 or 1, indicating if the horizon timestamp to be predicted belongs to a national holiday.

The first trainable operator of our model is a non-linear conditional block [43], which conditions the input $P_{ld}(t)$ with the exogenous variables $\mathbf{u}(t)$ at each step t :

$$\mathbf{g}(t) = \text{ReLU}(\text{MLP}_p(P_{ld}(t)) + \text{MLP}_u(\mathbf{u}(t))) \quad (28)$$

where MLP_p and MLP_u are Multi-Layer Perceptrons (MLPs) with a single hidden layer, ReLU activation function and a linear output layer. Both hidden and output layers have the same size k .

From the aforementioned block, we obtain a sequence of w k -dimensional vectors $\{\mathbf{g}(t-w+1), \dots, \mathbf{g}(t-1), \mathbf{g}(t)\}$ that are directly processed by our temporal encoder composed of 2 stacked recurrent layers with GRU cells. To produce the model output, the last cell state $\mathbf{s} \in \mathbb{R}^k$ is processed by a final MLP_y layer, with F -dimensional hidden layer and ReLU activations, which produces the prediction $\hat{\mathbf{y}}(t) \in \mathbb{R}^h$ for all horizon timesteps.

$$\hat{\mathbf{y}}(t) = \text{MLP}_y(\mathbf{s}) \quad (29)$$

This describes our standard MIMO model for load forecasting, in which the target to be predicted is the vector $\mathbf{y}(t) \in \mathbb{R}^h$:

$$\mathbf{y}(t) = [P_{ld}(t+1), P_{ld}(t+2), \dots, P_{ld}(t+h)] \quad (30)$$

For the evaluation of the MIMO predictor, we will use the simple strategy of post-processing its output, by taking $\max\{\hat{\mathbf{y}}(t)\}$ as input to the BESS control algorithm at each timestep t :

$$\hat{P}_{\text{pred}}(t) = \max\{\hat{\mathbf{y}}(t)\} \quad (31)$$

In line with our application, we also investigate a variant of the model which is optimized to predict directly only the peak load in the future horizon. The true prediction target and the predicted value of this model are simply:

$$y(t) = \max_{k \in \{1, \dots, h\}} P_{ld}(t+k) \quad (32)$$

$$\hat{P}_{\text{pred}}(t) = \hat{y}(t) \quad (33)$$

We will refer to this model as the PEAK predictor, in contrast with the MIMO predictor described above. Since the future peak is the only forecast needed, the PEAK predictor output can directly be used by the BESS control algorithm.

The described models are trained end-to-end for 150 epochs, using Stochastic Gradient Descent (SGD) with a batch size of 64 training examples [44]. We use the L1-loss with L2-regularization, which tries to keep model parameters small to mitigate overfitting on the training set:

$$\mathcal{L}(\hat{\mathbf{Y}}, \theta, \lambda) = \frac{1}{N} \sum_{i=1}^N \|\mathbf{Y}_i - \hat{\mathbf{Y}}_i\| + \lambda \sum_{j=1}^{N_\theta} \theta_j^2 \quad (34)$$

where \mathbf{Y}_i and $\hat{\mathbf{Y}}_i$ are the true and predicted values, respectively. N is the number of training examples, N_θ is the number of trainable parameters and λ is a hyperparameter to be tuned. We choose the Adam optimizer to minimize this prediction loss [45].

3. Pilot implementation

3.1. General system layout

The BESS of Arbon Energie AG is directly connected to the medium voltage side of a 110/17-kV transformer, as shown in Fig. 4. The BESS has power and energy ratings of 1.25 MW and 1.35 MWh, respectively. The maximum alternating current (AC) output power of BESS is also 1.25 MW, since the converter has similar output power rating. At the same bus of 17 kV, a feeder of the 17-kV distribution grid is connected representing the total load of Arbon city. Power quality meters connected to the 17-kV side of the 110/17-kV transformer provide near real-time load measurements with update intervals of some seconds.

The BESS technical characteristics are summarized in Table 1. The converter efficiency and the battery round-trip efficiency are assumed to be constant throughout the year. The SoC at the beginning of each day is needed for the optimal case, while it

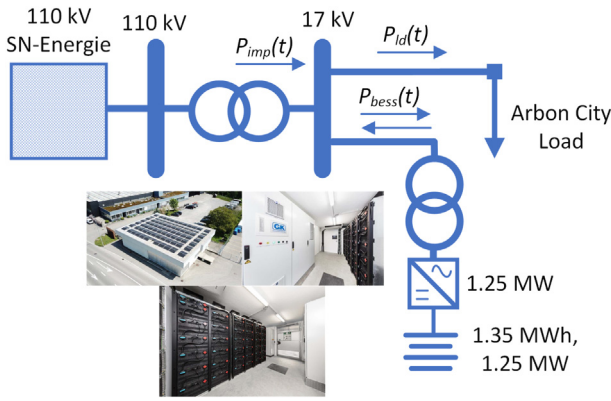


Fig. 4. Simplified schematic of the entire system.

Table 1

BESS technical characteristics.

Nominal energy capacity	1.35 MWh
Round-trip efficiency	92%
Converter efficiency	97.5%
Maximum charge/discharge power	1.25 MW
SoC range	7% to 93%
Initial SoC	93%
Energy throughput factor	0.9

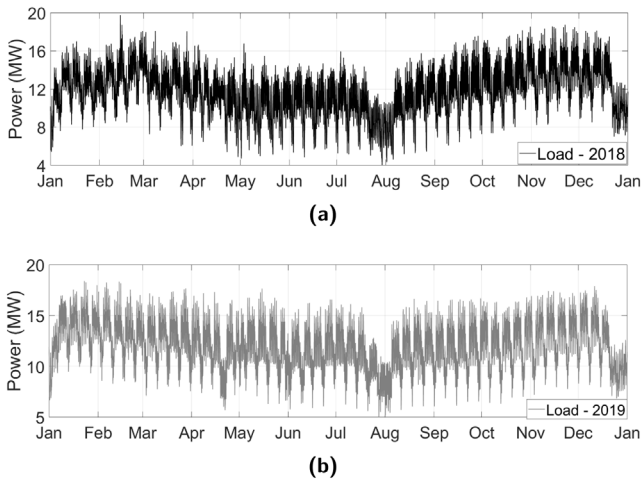


Fig. 5. Total load curve of Arbon in: (a) 2018, and (b) 2019.

is applied only at the first timestep for the control scheme. The energy throughput factor is used only for the optimal case and is based on the total usable SOC range that is equal to 86%. Since the BESS usable energy capacity per total charge is 86% of the nominal capacity, a factor of 0.9 is assumed due to possible partial charge cycles.

3.2. Load profile

Real data of the total load in the Arbon city are provided by Arbon Energie AG for the period 2018–2022 with time resolution of 15 min. Fig. 5 displays the total load profiles for 2018 and 2019, while similar curves are also used for the other years under assessment. As can be noticed, the maximum peaks on annual basis occur in January and February and range from 18 MW to 20 MW. Load valleys are also evident in August, December and January. The proposed BESS control scheme and the load forecasting model are assessed for the period 2019–2022.

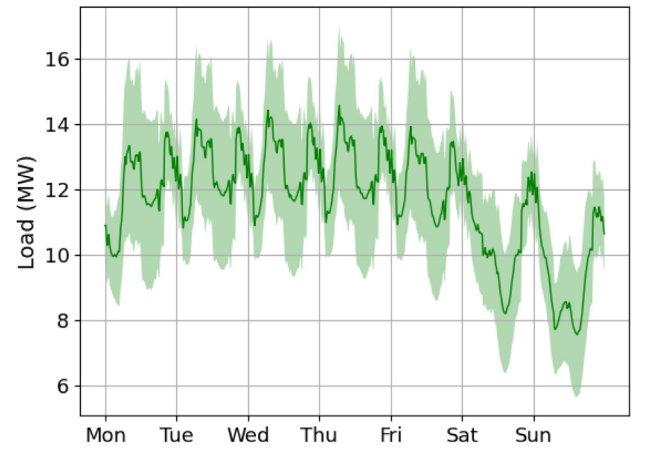


Fig. 6. Weekly distribution of load data in the city of Arbon. The green line represents the 15-min mean, while the shaded area spans one standard deviation above and below the 15-min mean.

For a better understanding of the data to be predicted, Fig. 6 displays the statistics of a week of power load, where the 15-min mean corresponds to the average of all 15-min values for the specific time and day of all examined years. Each day is usually characterized by two peaks, one in the morning and one in the afternoon, but it is not always clear which will be the highest one. The weekend is characterized by lower average consumption.

3.3. Inputs and assumptions

The effect of progressively adding more training data on performance is also investigated. In this context, four test evaluations are performed on different years: 2019, 2020, 2021 and 2022 (up to the 30th of June). A whole year of data to test is used in order to have a reliable and significant performance estimation, without biasing our analysis on specific months of the year. In each test year scenario, the previous years are considered as training data. A small part of these previous years, equivalent to roughly two months, is used as validation set to monitor performance while training. We use this validation set also to prevent overfitting, by performing early-stopping of the training process when validation error starts increasing. This was particularly helpful when training data is scarce. As shown in Fig. 7, in the test case of 2019, the training loss decreases much more than the validation loss. The best validation performance is achieved by stopping at around epoch 25. In contrast, in the test case of 2022, the discrepancy between training and validation loss is smaller and the model can be trained for longer without too much overfitting.

For the forecasting models, the only data required is the electric load time-series. Since our data is sampled every 15 min we assume $w = h = 96$, which corresponds to 24 h. The selection of 24 h as prediction window is based on the specific application of peak shaving, where the monthly peak power is of utmost importance. Longer prediction horizon periods can lead to higher forecasting errors, while shorter ones may lead to more than daily cycles for the BESS in case of multiple threshold changes. A window of 24 h was found to be sufficient, after evaluating many criteria, such as model complexity and simulation time. A larger past window would not lead to large gains in forecasting accuracy, while it would make the model more computationally expensive.

The Python library torch-spatiotemporal was used to define and train our models [46]. All experiment metadata and results were tracked using neptune.ai [47]. Table 2 summarizes our choices for the model hyperparameters. They were found via

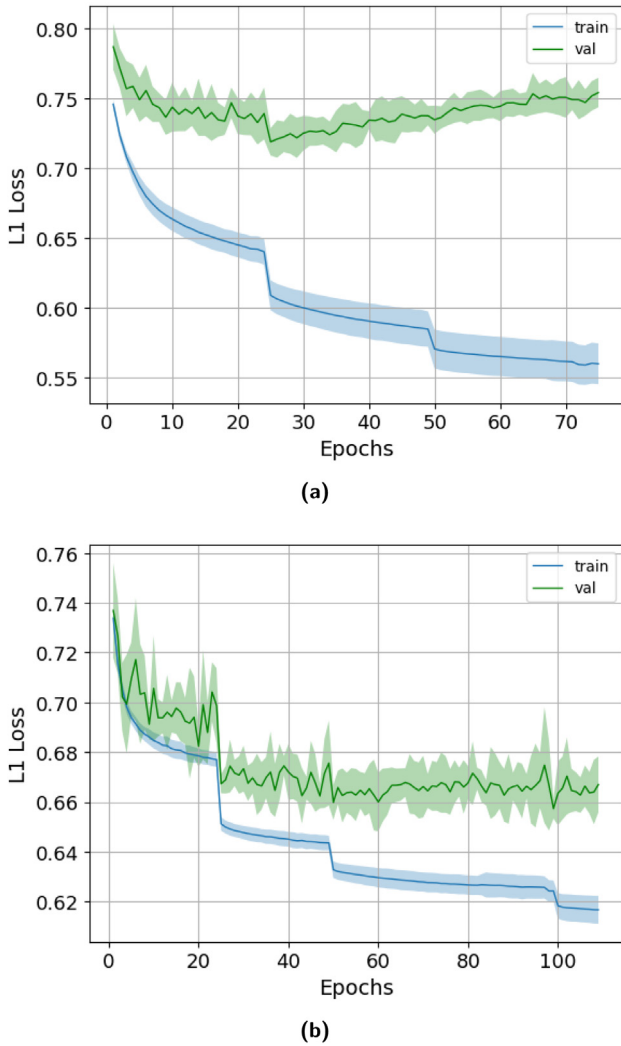


Fig. 7. Learning curves showing the average and standard deviation from 10 independent training runs of the MIMO forecasting model in: (a) 2019, and (b) 2022.

Table 2
Hyperparameters tuning.

Hyperparameters	Values	Optimal value
Number of GRU layers	1, 2, 3	2
Number of hidden layers in readout MLP _y	1, 2	1
Conditional block hidden layer size k	64, 128, 256	128
Readout MLP _y hidden layers size F	64, 128, 256	128
L2 regularization λ	0.0003, 0.001, 0.0015, 0.003	0.0015
Learning rate η	0.0003, 0.001, 0.003	0.003
Batch size	32, 64	64

search over a combination of the possible values by considering the validation error and trying to keep a reasonable balance between performance and model complexity. The chosen hyperparameters result in roughly 261k and 249k trainable parameters, for the MIMO predictor and PEAK predictor, respectively. We also employ a multi-step scheduler, which reduces the learning rate η by 25% when reaching epochs 25, 50 and 100.

The EPEX Spot price profiles are given by [48], while the c_{peak} and c_{use} are 9 CHF/kW and 10 CHF/MWh, respectively [49]. The

Table 3

Peak load forecasting results, reported as mean and standard deviation over 10 training runs.

Year	Strategy	MAE (MW)	MAPE (%)	NRMSE (%)	R ² (-)
2019	PEAK	0.725 ± 0.014	5.09 ± 0.10	9.91 ± 0.18	0.792 ± 0.007
	MIMO	0.902 ± 0.041	6.01 ± 0.26	12.27 ± 0.49	0.681 ± 0.025
2020	PEAK	0.639 ± 0.027	4.67 ± 0.21	8.12 ± 0.31	0.820 ± 0.014
	MIMO	0.696 ± 0.029	4.78 ± 0.20	8.56 ± 0.34	0.800 ± 0.016
2021	PEAK	0.595 ± 0.011	4.19 ± 0.10	8.16 ± 0.15	0.866 ± 0.005
	MIMO	0.822 ± 0.018	5.51 ± 0.11	11.07 ± 0.22	0.754 ± 0.009
2022	PEAK	0.537 ± 0.020	3.81 ± 0.15	10.43 ± 0.45	0.782 ± 0.019
	MIMO	0.829 ± 0.037	5.73 ± 0.24	15.08 ± 0.57	0.544 ± 0.035

1-min timestep is used for the simulation of each year, thus, the load data given by Arbon Energie AG are linearly interpolated within the 15-min time interval. The simulations are conducted with the software MATLAB 2018b. Finally, the MILP problem is formulated using the YALMIP toolbox [50] and is solved with CPLEX 12.9.0 [51].

3.4. Assessment criteria

Both technical and economical criteria are utilized for the assessment of the proposed BESS control scheme.

For the evaluation of peak load forecasting, the Mean Absolute Error (MAE), Mean Absolute Percentage Error (MAPE), Normalized Root Mean Square Error (NRMSE) and R² are reported. These metrics are commonly used for load forecasting and other time series prediction tasks. A detailed explanation of the metrics is given in [34].

For the technical assessment of BESS control scheme, monthly peak shaving is measured for each year, since it is used for the DSO's monthly power cost. Furthermore, the absolute average deviation (AAD) of monthly peak shavings from the optimal ones is computed in MW for each year. The AAD provides a better comparison of the annual method performance with respect to optimal peak shaving. Concerning the BESS operation, various criteria are evaluated with regards to the BESS utilization. Particularly, the number of cycles, daily energy throughput E_{thr} , $P_{\text{bess}}(t)$ range, BESS losses and annual degradation year $L_{\text{bess}}(a)$ are computed.

Finally, from the DSO's financial perspective, the cost savings from peak power C_{peak} , energy procurement C_{epex} , network usage C_{use} , as well as the total cost savings are assessed.

4. Results and analysis

4.1. Load forecasts

Table 3 summarizes the performance of peak load forecasting, divided by year and comparing the two models, MIMO, and PEAK.

The positive effect of adding more years of training data is evident in both MAE and MAPE, as there is a significant improvement from 2019 to 2022. It is also noticeable that the PEAK model, which focuses only on the prediction of the future peak, performs better than the standard MIMO strategy. This could be expected, as the standard MIMO predictor has to learn how to predict the full curve of future load, at the expense of higher errors at the peak value.

To facilitate the comparison with [34] and other research on load forecasting, the performance of the MIMO strategy on the full load curve is also reported in Table 4. In terms of the R² metric, the trend of increasing performance with additional training data can also be noticed. Nevertheless, the trend is less obvious than in Table 3, with a big improvement only from 2019

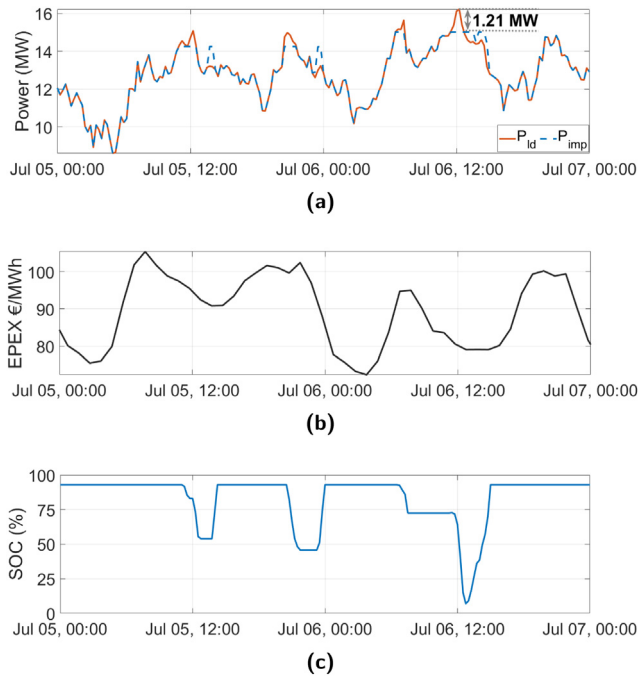


Fig. 8. Optimal results on 05-07 July 2021: (a) Measured power load and power load with BESS operation, (b) EPEX Spot price, and (c) SoC of BESS.

Table 4

Full load curve forecasting results, reported as mean and standard deviation over 10 training runs.

Year	MAE (MW)	MAPE (%)	NRMSE (%)	R ² (-)
2019	0.769 ± 0.010	6.89 ± 0.09	6.81 ± 0.10	0.359 ± 0.023
2020	0.724 ± 0.008	6.84 ± 0.09	6.02 ± 0.06	0.459 ± 0.015
2021	0.729 ± 0.005	6.88 ± 0.07	6.28 ± 0.04	0.502 ± 0.004
2022	0.788 ± 0.006	7.68 ± 0.07	7.51 ± 0.05	0.505 ± 0.007

to 2020. On average, the MIMO model has good performance when predicting the future 96 values, but the MAE values of Table 4 are always lower than the ones reported in Table 3 for MIMO, which refer to the day-ahead peak value. This suggests again how the full load curve prediction of MIMO is not suited at predicting the peak with maximum accuracy.

4.2. BESS technical assessment

As displayed in Fig. 8, the optimal case can achieve peak shavings of 1.21 MW on 06th July 2021, since a perfect load prediction is considered. In addition, the BESS maintains the peak power on 06th July 2021 at the level of the previous day. The BESS also follows an energy arbitrage strategy by discharging on high EPEX Spot prices and charging on low prices in order to minimize the energy procurement cost in the objective function. It is also evident that the BESS follows a complex SoC pattern due to various charging and discharging modes for the displayed days in July.

On the other hand, the proposed technique results in a straightforward SoC pattern, as depicted in Fig. 9. Particularly, the BESS discharges only when the upper threshold and the previous monthly peak are reached, and charges without exceeding the previous monthly peak. The BESS keeps a high SoC level so as to have sufficient energy capacity for the next peak load. It is clear that the control scheme cannot always achieve the optimal peak shaving, since the upper threshold depends on the day-ahead peak load forecast. In addition, the charging cycles can be

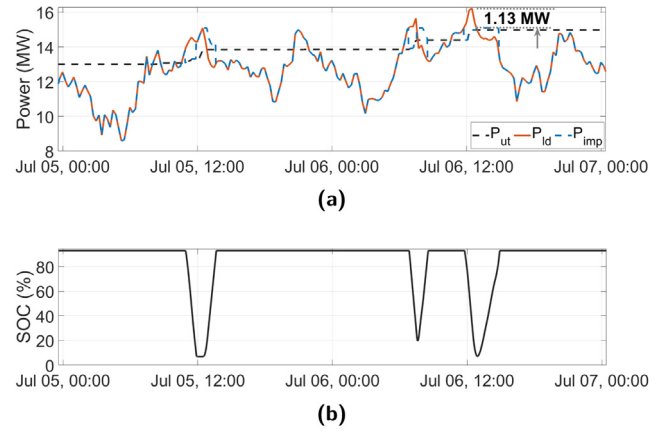


Fig. 9. Results applying the BESS control scheme on 05-06 July 2021: (a) Measured power load and power load with BESS operation, and (b) SoC of BESS.

conducted under high load conditions, as the goal is to always keep the BESS at high SoC levels in order to encounter the next power peak. From the economic perspective, the EPEX Spot price is not considered for the charging cycles, since a price forecast model is not developed in this study.

In terms of the monthly peak shaving, Table 5 shows the results of each year under assessment in the optimal case, as well as when applying the control scheme with the use of PEAK and MIMO forecasts. In the optimal case, it is evident that maximum peak shavings of 1.25 MW cannot always be achieved, as the optimization aims to minimize the total operation cost including both power and energy cost components. In particular, peak shaving can be partially limited in case that the EPEX Spot price variations lead to reduction of energy procurement cost. When the control scheme is applied, the peak shavings can have higher fluctuations than the optimal case, ranging from 0 MW to 1.25 MW. It is evident that when using the PEAK forecasts smaller deviations can be achieved for the examined period. Apart from the year of 2020, where the AAD increase, the AAD decreases over time. This can also be an indication that the use of additional historical data for retraining the load forecasting model can improve the accuracy of monthly peaks, and hence, the performance of the proposed BESS control scheme.

Table 6 summarizes the main technical outcomes from the simulation of each year under assessment. The BESS control scheme based on forecasts of either day-ahead load curve or peak load leads to considerably lower BESS utilization compared to the optimal case. The main reason of this behaviour is that the proposed technique focuses exclusively on the reduction of power peaks and not on the reduction of energy costs. On the other hand, the theoretical optimum is defined considering the EPEX Spot price profile, therefore, the optimal BESS operation combines both peak shaving and energy arbitrage strategies. The annual equivalent number of cycles when applying the control scheme is less than half of the respective value for the optimal case. Similar conclusions can be drawn with respect to the average daily energy throughput, annual BESS losses, and maximum BESS power. Concerning the annual BESS ageing, it is also evident that the proposed method results in lower battery degradation. Furthermore, an average annual BESS degradation of 2.06% can lead to a capacity depletion of about 20% after almost 11 years of operation. Hence, when an end-of-life (EoL) criterion of 80% is assumed for the remaining battery capacity, the proposed method can be applied for up to 10 years without any BESS upgrades. Moreover, the partial BESS utilization when applying the proposed control scheme enables the provision of additional services, e.g., frequency response and energy balancing.

Table 5

Monthly peak shaving in MW for each year under assessment.

Use case	Year	Jan	Feb	Mar	Apr	May	Jun	Jul	Aug	Sep	Oct	Nov	Dec	AAD
Optimal case	2019	1.25	1.12	1.25	1.08	1.25	1.20	1.24	0.99	1.17	0.86	1.11	1.05	–
	2020	0.88	1.25	0.87	1.23	1.10	1.25	1.09	1.24	0.86	0.95	1.23	0.89	–
	2021	0.91	0.95	1.25	1.25	1.25	0.92	1.21	1.19	0.91	0.86	0.94	0.88	–
	2022	0.81	0.84	1.22	0.95	0.92	1.22	–	–	–	–	–	–	–
Control scheme using MIMO	2019	1.25	1.02	1.25	0.43	0.00	0.54	0.46	0.00	0.00	0.16	0.74	0.20	0.63
	2020	0.00	0.72	0.56	0.48	0.01	0.79	0.67	0.00	0.00	0.31	0.76	0.57	0.66
	2021	0.32	0.00	1.25	1.25	0.18	0.24	1.04	0.79	0.13	0.25	0.05	0.31	0.56
	2022	0.46	0.40	1.01	0.71	0.20	0.88	–	–	–	–	–	–	0.38
Control scheme using PEAK	2019	1.25	0.99	1.25	0.43	0.00	0.55	0.46	0.00	0.00	0.73	0.69	0.19	0.59
	2020	0.00	0.72	0.56	0.48	1.25	0.88	0.44	0.00	0.00	0.31	0.84	0.65	0.58
	2021	0.66	0.37	1.25	1.25	0.18	0.26	1.13	0.79	0.16	0.32	0.05	0.20	0.49
	2022	0.52	0.58	1.12	0.71	0.80	0.88	–	–	–	–	–	–	0.22

Table 6

Summary of BESS technical results on annual basis.

BESS characteristic	Optimal case				Control scheme - MIMO				Control scheme - PEAK			
	2019	2020	2021	2022	2019	2020	2021	2022	2019	2020	2021	2022
Number of full cycles	324	328	329	160	77	43	57	33	61	37	53	31
E_{thr} (MWh)	1.20	1.17	1.14	1.20	0.29	0.16	0.20	0.25	0.23	0.13	0.19	0.24
$P_{bess}(t)$ (MW)	[–1.251.25]				[–1.251.25]				[–1.251.25]			
BESS losses (MWh)	56.3	58.2	59.4	27.9	11.9	6.8	9.1	5.1	9.4	5.9	8.5	4.8
$L_{bess}(a)$ (%)	3.23	3.24	3.16	2.02	2.07	2.05	2.05	1.17	2.07	2.05	2.06	1.17

Table 7

Annual savings on cost components from BESS operation.

Savings (kCHF)	Optimal case				Control scheme - MIMO				Control scheme - PEAK			
	2019	2020	2021	2022	2019	2020	2021	2022	2019	2020	2021	2022
C_{peak}	122	115	113	54	54	44	52	33	59	55	59	42
C_{epex}	0.2	0.9	0.5	0.1	–0.6	–0.3	–0.8	–0.3	–0.5	–0.3	–0.7	–0.3
C_{use}	4	4	4	2	0.9	0.5	0.7	0.4	0.7	0.5	0.6	0.4
C_{tot}	126	120	117	56	55	44	52	33	59	55	59	42

4.3. BESS economic assessment

The economic assessment is also conducted for the period 2019–2022 including the first six months of 2022. As shown in Table 7, the optimal annual savings range from 126k in 2019 to 117k in 2021, while at the first half of 2022 total savings of 56k could be achieved. It is remarkable that peak shaving can lead to the major part of the annual savings, while the savings on energy costs are negligible. Furthermore, in our study, emphasis is given on peak shaving for improved grid operation, since the use of network assets for decrease in energy purchase costs is not allowed according to the unbundling rules for network operators. Therefore, we aim at decreasing the power peaks, while not deteriorating the energy costs. When applying the control scheme, the relative savings from peak shaving compared to the optimal ones increase year by year apart from the year of 2020. The decline in BESS performance in 2020 is due to the lower accuracy of load forecasts due to changes in load patterns caused possibly by the COVID-19 restrictions. In particular, the relative savings from peak shaving increase from 44% in 2019 to 62% in 2022 when using the day-ahead load curve forecast. Moreover, the respective values with the use of day-ahead peak load forecast range from 48% in 2019 to 78% in 2022. The gradual improvement in annual savings also indicates that the retrained load forecasting models can also have a significant impact on the performance of the proposed BESS control scheme. It is evident that the control scheme shows better performance in combination with the day-ahead peak load forecast. Besides that, the proposed BESS operation does not lead to additional charges due to the energy purchase, though the algorithm does not consider the EPEX Spot price profile. In terms of the network usage costs, it is noticeable that the BESS can also lead to savings, since the charging cycles

do not result in additional energy costs for the operator. However, the BESS can achieve low savings due to the low network usage tariff both in the optimal case and when applying the control scheme.

4.4. Sensitivity analysis

The sensitivity analysis evaluates the impact of load forecasting error and time resolution of transformer measurements on the total savings.

To investigate the sensitivity of BESS control scheme to the forecasting error, the economical savings from peak shaving are computed while adding white Gaussian noise to the predictions from the PEAK model. The noise added using multiple standard deviations, simulates the effect of having increasingly poor predictors coupled with the control scheme. Noise signals with zero mean and variance ranging from 0.006 MW to 1 MW are added during simulations, corresponding to MAE ranging from 0.519 MW to 1.085 MW and relative measure of MAPE ranging from around 3.64% to 7.54%.

Fig. 10 shows clearly the effects of increasingly poor forecasting accuracy. As expected, adding a lot of noise leads to a sharp decline in peak shaving performance. In particular, the highest drop seems to appear when the MAE goes above 0.7 MW, corresponding to added noise with 0.55 MW of standard deviation, and above that level the performance deteriorates rapidly. This is expected, and shows the importance of peak prediction for the correct functioning of the control scheme. The proposed method is robust to smaller degradations in MAE, with performance mostly being stable or even improving for the first 5 noise levels. It can be concluded that the control scheme is robust with respect to peak prediction, provided the MAE remains roughly

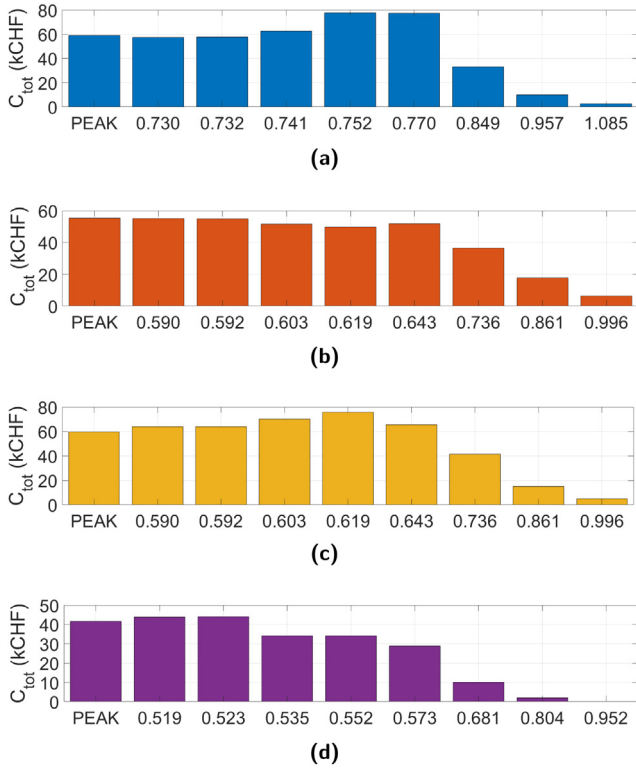


Fig. 10. Total savings using predictions from PEAK model including Additive White Gaussian Noise with MAE ranging from 0.519 MW to 1.085 MW: (a) 2019, (b) 2020, (c) 2021, and (d) 2022.

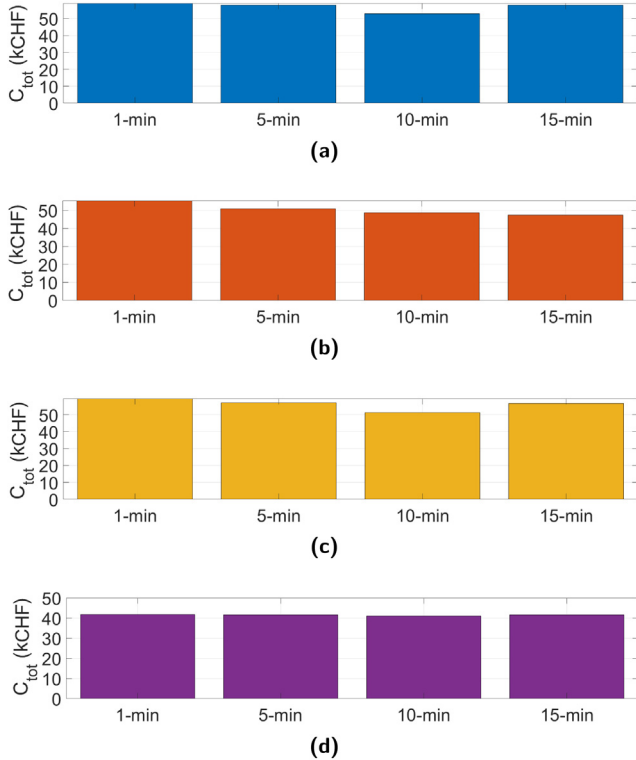


Fig. 11. Total savings utilizing transformer measurements with time resolution of [1, 5, 10, 15] min in: (a) 2019, (b) 2020, (c) 2021, and (d) 2022.

below 0.7 MW, or MAPE lower than 6%. Hence, it is doable to achieve such level of performance in peak magnitude predictions, using standard machine learning models for time series forecasting. Therefore, this performance could be easily replicated in other scenarios.

At the next step, different time resolutions of transformer measurements are utilized for the examined period. As displayed in Fig. 11, slight improvements on total cost savings are achieved with higher time resolutions. In 2019 and 2021, the provision of measurements every minute can reach up to 6k CHF increase on savings compared to the case of 10-min time resolution. In 2020, the improvement with 1-min time resolution can reach up to about 8k CHF, or around 15% in comparison to the 15-min one. In this case, the performance deterioration due to the lower load forecast accuracy can be partially compensated with higher time resolution. In 2022, it is evident that the high performance of the BESS control scheme cannot be additionally improved with higher time resolutions. Besides that, there is not a clearly ascending trend on savings by increasing the time resolution, since 15-min measurements may lead to approximately similar results with the 1-min measurements.

4.5. Discussion

The forecasting model can be fine-tuned at frequent time intervals, collecting new data over time and using it for model adaptation. More drastic long-term changes of the load profile due to the gradual integration of renewable energy resources and flexible loads, e.g. heat pumps and electric vehicles, could also be handled easily via model re-training.

In our study, the BESS control scheme is used only for peak shaving purposes. In fact, the unit is sometimes also utilized for ancillary services, therefore, the coordination with other methods is also required for a more realistic approach. In particular, the proposed method aims to keep the SoC at the highest possible level for the investigated period, though this assumption is not optimal when the BESS is used for frequency response services. On the contrary to the optimal case, the BESS charging mode is independent from the EPEX price, therefore, the energy procurement cost may have a slight rise. In case of existing EPEX price forecast, the BESS charging periods could also be adjusted only when the EPEX price is low so that the respective cost also decreases. However, it should be highlighted that in Switzerland and also in other countries a BESS cannot be utilized for energy arbitrage applications by the DSO due to unbundling requirements. Further analysis for a longer time horizon considering more details about capital, installation and operational costs could also provide insights about the viability of stationary BESS investments for peak shaving.

In terms of the sensitivity analysis, the slight increase in performance with some small noise levels, indicates a complex non-linear coupling between prediction and peak shaving performance. One hypothesis is that the maximum error might actually be more problematic than the average one, with poor performance concentrated on days with unluckily high prediction inaccuracies. The small noise might actually reduce high forecasting errors, though it degrades the prediction performance on average, as measured by the decreasing MAE. This complex relationship between peak prediction performance and control of peak shaving could be further investigated in another study.

5. Conclusions and future work

In this paper, a rule-based BESS control scheme based on day-ahead load predictions for peak shaving is examined. The BESS operation depends on the day-ahead load prediction, the

real-time transformer measurement and the peak power of the previous timesteps of the month. In contrast to previously published peak shaving approaches, the presented method is robust against forecast deviations and utilizes the battery storage less than optimization-based methods.

Regarding the forecasting model, a non-linear deep learning predictor based on a GRU-RNN shows promising forecasting performance. In particular, the PEAK predictor achieves forecasts of higher accuracy than recurrent forecasting models that predict the full load curve. Leveraging multiple years of data, the accuracy of load forecasts can increase by periodically retraining the model and adapt it to the new test conditions.

Concerning the BESS control scheme, the relative savings from peak shaving can increase year by year ranging from 48% in 2019 to 78% in 2022 compared to the theoretical optimum with perfect forecast. Moreover, the BESS can achieve higher savings with the PEAK predictor than the MIMO predictor indicating that peak shaving operation needs to be based on peak load prediction and not on full load curve prediction. The proposed control algorithm does not also cause negative effects on the costs related to energy procurement and network usage fees. In addition, the control scheme leads to annual battery ageing rate of 2%, leaving space for further BESS utilization in the context of other services.

The sensitivity analysis has shown that the BESS control scheme is robust against load prediction errors. In particular, the method performance is mostly stable or even improved for MAE levels below 0.7 MW, or MAPE lower than 6%. It is also concluded that in case of low prediction accuracy the higher time resolution of transformer measurements can improve up to about 15% the total savings in 2020. Nevertheless, there is not always an improvement on cost savings by increasing the time resolution.

The proposed control scheme can be continuously evaluated. In order to bridge the gap with the optimal case, other forecasting models could also be investigated, considering additional input data, e.g., weather data. Finally, online model adaptation could be investigated, to understand if periodic full-dataset re-training might be avoided by continuously fine-tuning the model on new test data.

CRedit authorship contribution statement

Nikolaos A. Efkarpidis: Conceptualization, Methodology, Software, Formal analysis, Investigation, Writing – original draft, Writing – review & editing. **Stefano Imoscopi:** Conceptualization, Methodology, Software, Formal analysis, Investigation, Writing – original draft, Writing – review & editing. **Martin Geidl:** Conceptualization, Methodology, Writing – review & editing, Supervision. **Andrea Cini:** Conceptualization, Methodology, Investigation, Writing – review & editing. **Slobodan Lukovic:** Writing – review & editing, Supervision. **Cesare Alippi:** Writing – review & editing, Supervision. **Ingo Herbst:** Resources, Writing – review & editing, Supervision.

Declaration of competing interest

The authors declare that they have no known competing financial interests or personal relationships that could have appeared to influence the work reported in this paper. The content and views expressed in this material are those of the authors and do not necessarily reflect the views or opinion of the ERA-Net SES initiative. Any reference given does not necessarily imply the endorsement by ERA-Net SES.

Data availability

The data that has been used is confidential.

Acknowledgements

This work is developed within the project “Service Optimization of Novel Distributed Energy Regions” funded by the Swiss Federal Office of Energy SFOE and the joint programming initiative ERA-Net Smart Energy Systems’ focus initiative Integrated, Regional Energy Systems, with support from the European Union’s Horizon 2020 research and innovation programme under Grant Agreement No. 775970. The authors would like to thank SFOE, the joint programming initiative ERA-Net Smart Energy Systems, as well as the industrial partners in the project, Siemens Switzerland AG and Arbon Energie AG, for the provision of technical data that were significant for the accomplishment of this study.

References

- [1] V. K. Mehta, R. Mehta, Principles of Power System, fourth ed., S. Chand, New Delhi, India, 2005, pp. 1–608.
- [2] MIT, The Future of the Electric Grid, Technical report, 2011, pp. 1–268.
- [3] A. Nourai, V.I. Kogan, C.M. Schafer, Load leveling reduces T&D line losses, *IEEE Trans. Power Deliv.* 23 (4) (2008) 2168–2173.
- [4] M. Uddin, M.F. Romlie, M.F. Abdullah, S. A. Halim, A.H. A. Bakar, T. C. Kwang, A review on peak load shaving strategies, *Renew. Sustain. Energy Rev.* 82 (Part 3) (2018) 3323–3332.
- [5] S.V. Berg, A. Savvides, The theory of maximum kW demand charges for electricity, *Ener. Econ.* 5 (4) (1983) 258–266.
- [6] A.S. Brouwer, M. V. D. Broek, W. Zappa, W.C. Turkenburg, A. Faaij, Least-cost options for integrating intermittent renewables in low-carbon power systems, *Appl. Energy* 161 (2016) 48–74.
- [7] F.H. Magnago, J. Alemany, J. Lin, Impact of demand response resources on unit commitment and dispatch in a day-ahead electricity market, *Int. J. Electr. Power Energy Syst.* 68 (2015) 142–149.
- [8] P.D. Lund, J. Lindgren, J. Mikkola, J. Salpakari, Review of energy system flexibility measures to enable high levels of variable renewable electricity, *Renew. Sustain. Energy Rev.* 45 (2015) 785–807.
- [9] F. Gangale, J. Vasiljevska, C.F. Covrig, A. Mengolini, G. Fulli, Smart Grid Projects Outlook 2017, Technical report, 2017, pp. 1–91.
- [10] A. Rahimi, M. Zarghami, M. Vaziri, S. Vadhva, A simple and effective approach for peak load shaving using Battery Storage Systems, in: 45th Nor. Amer. Pow. Symp. (NAPS), 2013, pp. 1–5.
- [11] K.C. Divya, J. Østergaard, Battery energy storage technology for power systems—An overview, *Electr. Power Syst. Res.* 79 (4) (2009) 511–520.
- [12] M. Koller, T. Borsche, A. Ulbig, G. Andersson, Review of grid applications with the Zurich 1 MW battery energy storage system, *Electr. Power Syst. Res.* 120 (2015) 128–135.
- [13] M. Bachmann, A. Bürki, A. Bifare, M. Eisenreich, F. Felix, M.G. Vayá, M. Früh, P. Hauser, F. Kienzle, J. Müller, Smart Grid findet statt – eine Übersicht, *Energienetze Dossier* 5 (2017) 20–24.
- [14] S. Kieber, Arbon energie AG batteriespeichersystem (BESS), 2019, pp. 1–21.
- [15] F. Braeuer, J. Rominger, R. McKenna, W. Fichtner, Battery storage systems: An economic model-based analysis of parallel revenue streams and general implications for industry, *Appl. Energy* 239 (2019) 1424–1440.
- [16] F. Baumgarte, G. Glenk, A. Rieger, Business models and profitability of energy storage, *IScience* 23 (10) (2020) 1–12.
- [17] M. Shin, S. So, K. Kim, A control approach of battery energy storage systems to reduce kW demand, in: MATEC Web of Conf. (ICIEA), Vol. 68, 2016, pp. 1–5.
- [18] M. Ehsan Raoufat, B. Asghari, R. Sharma, Model predictive BESS control for demand charge management and PV-utilization improvement, in: IEEE Pow. and Ener. Soc. Innov. Smart Grid Tech. Conf. (ISGT), 2018, pp. 1–5.
- [19] K.H. Chua, Y.S. Lim, S. Morris, Energy storage system for peak shaving, *Int. J. Energy Sec. Manag.* 10 (1) (2016) 3–18.
- [20] B.R. Ke, T.T. Ku, Y.L. Ke, C.Y. Chuang, H.Z. Chen, Sizing the battery energy storage system on a university campus with prediction of load and photovoltaic generation, *IEEE Trans. Ind. Appl.* 52 (2) (2016) 1136–1147.
- [21] A. Oudalov, R. Cherkaoui, A. Beguin, Sizing and optimal operation of battery energy storage system for peak shaving application, in: IEEE Lausanne PowerTech Proc., 2007, pp. 621–625.
- [22] V. Papadopoulos, J. Knockaert, C. Develder, J. Desmet, Peak shaving through battery storage for low-voltage enterprises with peak demand pricing, *Energies* 13 (5) (2020) 1–17.
- [23] M. Hosseina, S.M.T. Bathaee, Optimal scheduling for distribution network with redox flow battery storage, *Energy Convers. Manage.* 121 (2016) 145–151.
- [24] M. Rowe, T. Yunusov, S. Haben, C. Singleton, W. Holderbaum, B. Potter, A peak reduction scheduling algorithm for storage devices on the low voltage network, *IEEE Trans. Smart Grid* 5 (4) (2014) 2115–2124.

- [25] S.U. Agamah, L. Ekonomou, Peak demand shaving and load-leveiling using a combination of bin packing and subset sum algorithms for electrical energy storage system scheduling, *IET Sci., Meas. Technol.* 10 (5) (2016) 477–484.
- [26] Y. Levron, D. Shmilovitz, Power systems' optimal peak-shaving applying secondary storage, *Electr. Power Syst. Res.* 89 (2012) 80–84.
- [27] H. Pezeshki, P. Wolfs, G. Ledwich, A model predictive approach for community battery energy storage system optimization, in: *IEEE Pow. Ener. Soc. Gen. Meet. (PESGM)*, 2014, pp. 1–6.
- [28] E. Reihani, M. Motalleb, R. Ghorbani, L.S. Saoud, Load peak shaving and power smoothing of a distribution grid with high renewable energy penetration, *Renew. Energy* 86 (2016) 1372–1379.
- [29] A. Lucas, S. Chondrogiannis, Smart grid energy storage controller for frequency regulation and peak shaving, using a vanadium redox flow battery, *Electr. Power Energy Syst.* 80 (2016) 26–36.
- [30] C. Lu, H. Xu, X. Pan, J. Song, Optimal sizing and control of battery energy storage system for peak load shaving, *Energies* 7 (12) (2014) 8396–8410.
- [31] M. Rowe, T. Yunusov, S. Haben, W. Holderbaum, B. Potter, The real-time optimisation of DNO owned storage devices on the LV network for peak reduction, *Energies* 7 (6) (2014) 3537–3560.
- [32] E. Reihani, S. Sepasi, L.R. Roose, M. Matsuura, Energy management at the distribution grid using a Battery Energy Storage System (BESS), *Int. J. Electr. Power Energy Syst.* 77 (2016) 337–344.
- [33] C. Kuster, Y. Rezgui, M. Mourshed, Electrical load forecasting models: a critical systematic review, *Sustain. Cities Soc.* 35 (2017) 257–270.
- [34] A. Gasparin, S. Lukovic, C. Alippi, Deep learning for time series forecasting: The electric load case, *CAAI Trans. Intell. Technol.* 7 (1) (2022) 1–25.
- [35] J. Lee, Y. Cho, National-scale electricity peak load forecasting: Traditional, machine learning, or hybrid model? *Energy* 239 (2022) 122366.
- [36] S. Kumar, L. Hussain, S. Banarjee, M. Reza, Energy load forecasting using deep learning approach-LSTM and GRU in spark cluster, in: *2018 5th Inter. Conf. on Emer. Appl. of Infor. Tech. (EAIT)*, 2018, pp. 1–4.
- [37] VSE, Netznutzungsmodell für das schweizerische Verteilnetz – Grundlagen zur Netznutzung und Netznutzungsentschädigung in den Verteilnetzen der Schweiz, Technical report, 2021, pp. 1–85.
- [38] B. Xu, A. Oudalov, A. Ulbig, G. Andersson, D.S. Kirschen, Modeling of lithium-ion battery degradation for cell life assessment, *IEEE Trans. Smart Grid* 9 (2) (2018) 1131–1140.
- [39] E. R. Iglesias, P. Venet, S. Pelissier, Efficiency degradation model of lithium-ion batteries for electric vehicles, *IEEE Trans. Ind. Appl.* 55 (2) (2019) 1932–1940.
- [40] K. Cho, B. V. Merriënboer, D. Bahdanau, Y. Bengio, On the properties of neural machine translation: Encoder-decoder approaches, 2014, pp. 1–9, arXiv preprint [arXiv:1409.1259](https://arxiv.org/abs/1409.1259).
- [41] J. Chung, C. Gulcehre, K. Cho, Y. Bengio, Empirical evaluation of gated recurrent neural networks on sequence modeling, 2014, pp. 1–9, arXiv preprint [arXiv:1412.3555](https://arxiv.org/abs/1412.3555).
- [42] L. Kuan, Z. Yan, W. Xin, C. Yan, P. Xiangkun, S. Wenxue, J. Zhe, Z. Yong, X. Nan, Z. Xin, Short-term electricity load forecasting method based on multilayered self-normalizing GRU network, in: *IEEE Conf. on Ener. Inter. and Ener. Syst. Integ. (EI2)*, 2017, pp. 1–5.
- [43] A. Borovykh, S. Bohte, C.W. Oosterlee, Conditional time series forecasting with convolutional neural networks, 2017, pp. 1–22, arXiv preprint [arXiv:1703.04691](https://arxiv.org/abs/1703.04691).
- [44] S. Ruder, An overview of gradient descent optimization algorithms, 2016, pp. 1–14, arXiv preprint [arXiv:1609.04747](https://arxiv.org/abs/1609.04747).
- [45] D.P. Kingma, J. Ba, Adam: A method for stochastic optimization, 2014, pp. 1–15, arXiv preprint [arXiv:1412.6980](https://arxiv.org/abs/1412.6980).
- [46] A. Cini, I. Marisca, Torch spatiotemporal, 2022, Available [Online]: <https://github.com/TorchSpatiotemporal/tsl>.
- [47] neptune.ai, Neptune: experiment tracking and model registry, 2022, Available [Online]: <https://neptune.ai>.
- [48] Entsoe, Transparency Platform, Available [Online]: <https://transparency.entsoe.eu/>.
- [49] S.N. Energie, Informationspflicht der Netzbetreiber. Website, <https://www.snergie.ch/uebertragungverteilung/netztarife/>.
- [50] J. Löfberg, YALMIP: A toolbox for modeling and optimization in MATLAB, in: *IEEE Inter. Symp. on Comp.-Aid. Con. Syst. Des. (CACSD)*, 2004, pp. 284–289.
- [51] IBM, IBM ILOG CPLEX Optimization Studio, Available [Online]: <https://www.ibm.com/products/ilog-cplex-optimization-studio>.